CLM-R218

CLM-R218

UKAEA

Report

THE EFFECT OF SPUTTERING ON BEAM-HEATING IN INTOR

D. E. T. F. ASHBY
M. H. HUGHES

CULHAM LABORATORY
Abingdon Oxfordshire

1981

C18 Available from H. M. Stationery Office £2.00

CLM-R218

THE EFFECT OF SPUTTERING ON BEAM-HEATING IN INTOR

by

D E T F Ashby and M H Hughes

Culham Laboratory, Abingdon, Oxon, OX14 3DB,UK.

(Euratom/UKAEA Fusion Association)

ABSTRACT

This report was originally written for a reactor study carried out at Culham and was subsequently used in the INTOR study. Computer simulation is used to examine the effect on ignition in INTOR of ions sputtered from the walls during neutral beam heating.

21.10.81.

ISBN 0 85311 099 9

1. INTRODUCTION

This report examines the effect of impurity atoms on two representative beam-heating scenerios. The 1-D code HERMES[1] is used to model INTOR with a self-consistent sputtering model in which the escaping neutrals sputter iron atoms into the plasma. The intention is to illustrate the physical effects that are predicted by a typical computer model.

2. THE MODEL

Details of the computational model are described in the following sub-sections.

2.1. The Machine

The original INTOR dimensions and parameters are used namely:

Major radius R = 4.5m.

Equivalent minor radius a = 1.5m.

Toroidal current I = 4MA.

Toroidal magnetic field B_ϕ = 5 T

2.2. Plasma Transport

The INTOR reference transport is used to describe energy and plasma transport namely:

Electron thermal diffusivity $\chi_e = \frac{5\times10^{19}}{n_e}\ m^2 s^{-1}$ [Bohm if q<1]

Ion thermal diffusivity $\chi_i = 3\chi_i$ (neoclassical)

Plasma diffusivity $D = \frac{1}{4}\chi_e$ + neoclassical.

Note: Where neoclassical transport is included in the above expressions the off-diagonal terms are dropped excepting those associated with the Ware Pinch Effect.

2.3. Impurity Transport

The impurity transport is neoclassical with off-diagonal terms included (i.e. grad T). An additional anomalous term is added so as to be consistent with the anomalous plasma transport (i.e. $\frac{1}{4}\chi_e \frac{\partial n_I}{\partial r}$). The impurities are assumed to be in the intermediate Pfirsch-Schlüter regime. The expressions used are those given by Hirshman[2]. Note that impurity ions are allowed to escape at the plasma boundary; hence if the impurity influx is constant an equilibrium is approached where the influx and outflux of impurities balance.

The transport equations associated with the impurities are given below.

The total impurity density n_I is transported and the impurity flux is given by

$$\Gamma_I = D_I \frac{\partial n_I}{\partial r} + D_I^H \left[n_H \frac{\partial n_I}{\partial r} - \langle z \rangle n_I \frac{\partial n_H}{\partial r} \right] - \beta_I^H n_H n_I \frac{\partial T_H}{\partial r}$$

$$- D_I^I \left[\langle z^2 \rangle n_I \frac{\partial n_I}{\partial r} - \langle z \rangle n_I \frac{\partial}{\partial r} \left(\langle z \rangle n_I \right) \right] + \beta_I^I n_I^2 \frac{\partial T_H}{\partial r} \qquad (1)$$

The hydrogen flux is affected by the presence of impurities and becomes

$$\Gamma_H = D_H \frac{\partial n_H}{\partial r} + D_H^I \left[\langle z^2 \rangle n_I \frac{\partial n_H}{\partial r} - n_H \frac{\partial}{\partial r} \left(\langle z \rangle n_I \right) \right] + \beta_H^I n_H n_I \frac{\partial T_i}{\partial r} \quad \ldots(2)$$

The energy equipartion time is also affected by the presence of impurities and becomes

$$\frac{1}{\tau_{eq}} = \frac{3m_e}{n_e \tau_e} \left(\frac{n_H}{M_H} + \frac{n_I \langle z^2 \rangle}{M_I} \right) \qquad (3)$$

The diffusivities and associated parameters are as follows:

$$D_H^I = D_I^H = \frac{\rho_H^2 q^2}{n_H \tau_i}$$

ρ_H = hydrogen ion-gyro radius

q = safety factor

$$D_I^I = D_H^I \left(\frac{M_I}{2M_H} \right)^{\frac{1}{2}}$$

$D_I = D_H = \frac{1}{4}\chi_e$ the anomalous diffusivity.

$$\beta_H^I = \frac{D_H^I}{T_H} \left(-\tfrac{1}{2} \langle z^2 \rangle - \langle z \rangle \right)$$

$$\beta_I^H = \frac{D_I^H}{T_H}\left(-\tfrac{1}{2}\langle z\rangle - 1\right)$$

$$\beta_I^I = \frac{D_I^I}{T_H}\left(\langle z^2\rangle - \langle z\rangle^2\right).$$

The suffix I refers to the impurity species while the suffix H refers to the hydrogenous species, which to simulate a D-T mixture is taken to have an atomic mass of 2.5. This model assumes that the temperature of the impurity ions is the same as that of the hydrogenous ions. The values of z and its various averages are given by the radiation model which assumes coronal equilibrium.

2.4 Radiation

Tarter's average ion model for iron was used in the version of HERMES used in this work; later versions use Post's average ion model. The two models give similar results. (3)

2.5 Sputtering

The sputtering coefficient used to relate the influx of iron atoms to the energy and flux of escaping neutrals is due to Behrisch. (4) Note that this version of HERMES, unlike later versions, uses values of the sputtering coefficient appropriate for sputtering by hydrogen and not deuterium or tritium. However in the modelling to be described runs were repeated with the basic sputtering coefficient increased by factors from 1-10 to determine the sensitivity of the results to sputtering coefficient; the difference in sputtering yield from tritons compared with protons is about a factor two or three.

In the computer model iron atoms from the wall are deposited in the mesh cell closest to the wall. Twenty mesh points are used so the cell width is 7.5cm; the actual penetration distance expected is rather less namely 1-3 cm depending upon the edge density.

3. THE BEAM HEATING SCENARIOS

Two beam heating scenarios were used; both started from the same ohmic steady-state. The initial mean electron density was $0.53 \times 10^{20} m^{-3}$

giving 0.80 x 10^{20} m^{-2} as the value of $\bar{n}a$. This value should be compared with 1.35 x 10^{20} m^{-2} which is the minimum of the ignition curve given by HERMES with no impurities (see Fig.1). Thus in both scenarios beam-heating commenced at a point below the ignition curve and in the vicinity of the Murakami Limit $\left(\bar{n}_{20} \lesssim \frac{B(T)}{2R(m)} = 0.56\right)$. A 50MW mono-energetic pencil beam of deuterons was used to heat the plasma. In the first scenario the injection energy was 200keV. In this case the recycling coefficient for DT was taken as unity; hence the density increased during injection and the density profile tended to be flat-topped. In the second scenario the beam energy was 100keV and once the mean density reached 0.61 x 10^{20} m^{-3} the recycling coefficient was adjusted to maintain the density constant. In this case the density profile tended to be parabolic in shape because of the strong central particle source due to the beam.

The first scenario is representative of the heating methods commonly quoted for INTOR. The second scenario is representative of the low energy, low density approach.[5]

4. RESULTS

Fig.2 shows the variation of $\bar{\beta}$ against time for both scenarios, first with no sputtering and then with the sputtered flux multiplied by 1, 2, 4 and 10. To reiterate what is done; the energy distribution and flux of neutrals escaping from the plasma is determined by a Monte Carlo calculation; then the sputtering data given by Behrisch, for protons on iron as a function of energy, is used to determine the influx of iron atoms from the wall; finally this impurity flux is arbitrarily multiplied to determine the sensitivity of the final outcome to the sputtering model.

Although Fig.2 shows that the value of $\bar{\beta}$ is decreased due to the presence of sputtered iron it should be borne in mind that the target for ignition is $\bar{\beta} \gtrsim 3.5\%$ (see Fig.1). Once this value is exceeded the energy density in the plasma is sufficient for ignition as long as the radiation from the central plasma is low. If $\bar{n}a$ is too small for ignition, as in the second scenario, then in principle it is possible to turn off the beam and inject gas to achieve the required density. On the basis of Fig.2 one would say that sputtered iron will not prevent ignition in the first scenario but will in the second scenario if the sputtered flux is increased by a factor of more than two.

Fig. 3 illustrates the different radial profiles of n_e and n_I in the two scenarios and their effect on radiated power. In the first scenario, where a 200keV beam is used with unity recycling coefficient, the electron density profile is flat-topped with a large $\partial n_e/\partial r$ at the edge. This term, in competition with the $\partial T/\partial r$ term in the impurity diffusion (eqn. 1), results in the impurity density peaking at the edge of the plasma. In the second scenario the electron density is not flat-topped and $\partial n_e/\partial r$ is less near the edge; the net result is an essentially flat impurity density profile. The result of the differences in impurity distribution on the profiles of radiated power is marked and is further exaggerated by both the change in n_e and the variation of radiated power with temperature. (Remember that radiated power = $n_e n_z S(T)$ and for medium mass impurities, such as iron, $S(T)$ decreases rapidly once $T_e \gtrsim 200$eV.)

Fig.4 illustrates the effect that sputtered impurities have on the radiation losses. An example from the first scenario with unity recycling coefficient has been chosen where the total radiation loss is extreme. Two cases are compared; the first when there is no influx of sputtered iron; the second when the sputtered flux is increased by a factor ten. Sputtered impurities have a dramatic effect on the way the total plasma losses are partitioned; with no sputtering, less than 5% of the power is radiated compared with about 80% when iron is sputtered. However most of the radiation comes from the plasma edge (see Fig.3), consequently radiation plays a minor role in determining losses from the central plasma inside $r = 1.0$m.

Fig.5 compares the time dependence of the sputtered flux, and the resulting number of iron atoms within the plasma, for the two scenarios and shows the effect of changing the sputtering coefficient. In the first scenario the sputtered flux and the number of iron atoms is insensitive to the sputtering coefficient and both quantities are crudely constant. This result reflects the strong feed-back mechanism resulting from the sputtering model; if the 'edge' temperature is high then the influx of iron atoms is large, and, since impurities accumulate at the plasma edge and radiate strongly (see Fig.3) the 'edge' temperature falls. This effect is essentially absent in the second scenario where the recycling coefficient is adjusted to maintain the density constant. Again the reason is clear from Fig.3; since n_e and n_z are both comparatively small the plasma edge does not radiate strongly and the 'edge' temperature remains comparatively high. The value of the 'edge' temperature is critical since it determines the energy of

the escaping neutrals and thus the sputtered flux.

One measure of the effect of sputtering is to ask whether or not ignition occurs. This criterion, although simple to comprehend, is a very inefficient indication of the effect of sputtering. Whether or not ignition occurs depends critically on a number of competing mechanisms, and often calls for time-consuming computer runs. In addition the second class of scenarios, with $\bar{n}$ constant at $0.61 \times 10^{20} m^{-3}$, requires that the density be increased before ignition can possibly occur since $\bar{n}a$ is below the ignition curve for no impurities. However, for illustrative purposes some attention was paid to ignition. In the first scenario, which had E_B = 200keV and unity recycling coefficient, the cases with no sputtering and ordinary sputtering ignited. The other three cases with the sputtering coefficient multiplied by 2, 4 and 10 were not run for sufficient time to determine if the plasma would ignite. But, for these three cases, Fig.2 shows that $\bar{\beta}$ was increasing with time and ignition could be expected inside 10s for all but the last case.

An attempt was made to ignite one of the constant density scenarios by switching off the beam and increasing the density. The case chosen had the sputtering coefficient multiplied by a factor two. To achieve ignition it was necessary to increase the beam power from 50MW to 60MW. Fig.6 illustrates this case and shows profiles of n_e and n_I as the density is increased.

A new phenomenon is apparent from Fig.6. When the beam is switched off at 6.5s the profiles of n_e and n_z are similar to those already shown in Fig.3. When gas is injected at the plasma boundary the electron density inverts, as expected, and the change in $\partial n_e/\partial r$ strongly affects the impurities. In the outer region of the plasma, where the sign of $\partial n_e/\partial r$ has reversed, the impurities diffuse outwards. At the same time the impurity flux from the wall drops because of the sudden reduction of the 'edge' temperatures as gas is injected. This trend is enhanced as more gas is injected at 7.5s and the net result is that the number of iron atoms in the plasma decreases from 2.8×10^{19} to 0.7×10^{19} in three seconds as the density is increased on the way to ignition.

Yet another effect was observed during this phase of the modelling. If the plasma density was increased too quickly the radiative losses

from the plasma edge exceeded the fusion power and the temperature profile commenced to collapse from the edge inwards. This effect is currently being studied.[6]

5. DISCUSSION AND CONCLUSION

Taken at their face value the results presented argue that radiation from sputtered impurities will not play a dominant role in INTOR; this conclusion would be misguided. What the results do argue is that, within the confines of the reference transport and the extra simplifications used in the computer model, then impurities do not appear to be overly troublesome. This distinction is not sheer pedantry. It is important to continually recall that the particle and thermal transport are uncertain both in magnitude and functional form as also is the radiated power. To get any one of these quantities 'right' to within 50% would be considered excellent agreement. In addition the model ignores toroidal geometry and stability. All that computer modelling of conceptual tokamak reactors can hope to do is to draw attention to possible effects, describe them qualitatively, help to elucidate the effects and determine their sensitivity to the parameters involved.

What the examples show is obvious once stated, namely that with the reference transport and radiation determined by simple coronal equilibrium the following results accrue.

(1) The sputtered impurities do not accumulate on the axis.

(2) Whether or not the sputtered impurities concentrate at the edge depends on the electron density profile which in turn depends on the recycling coefficient for hydrogen.

(3) Radiative losses tend to peak at the edge, where the temperature is low, and hence they have little effect on the losses from the central plasma where fusion occurs. This last statement is true only as long as the temperature profile does not collapse.

(4) Gas puffing can, by reversing the sign of $\partial n/\partial r$, cause the number of impurities to decrease.

(5) The feed-back between sputtered flux and 'edge' temperatures can result in the flux being insensitive to the magnitude of the sputtering coefficient.

REFERENCES

1. Details of HERMES are available on request.

2. HIRSHMAN, S.P. Phys. Fluids, 19, No.1, (1976) 155.

3. POST, D.E., JENSEN, R.V., TARTER, C.B., GRASBERGER, W.H. and LOKKE, W.A. Atomic Data and Nuclear Data Tables, 20, No.5, (1977) 397.

4. BEHRISCH, R. "Tokamak Reactors for Breakeven" Int.School of Fusion Reactor Tech. Erice (1976), Pergamon Press, (1978) 37.

5. ASHBY, D.E.T.F. and HUGHES, M.H. "A Neutral Beam-Heating Scenario for Energies of ∿ 100keV." Unpublished. Details available on request.

6. ASHBY, D.E.T.F. and HUGHES, M.H. Nuclear Fusion, 21, (1981) 911.

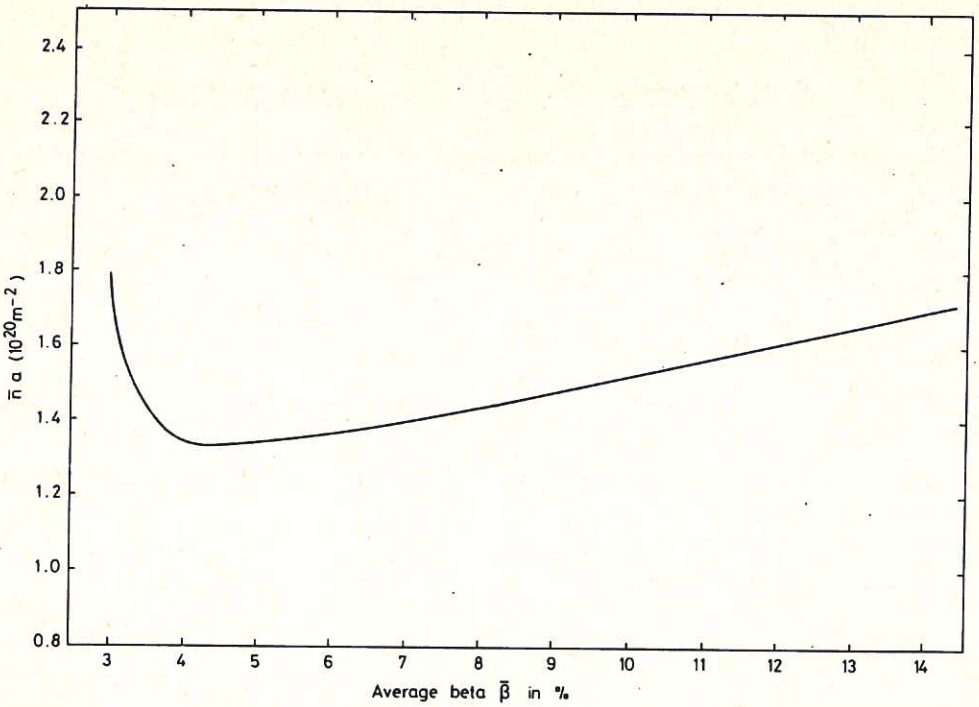

Fig.1 Ignition curve for INTOR showing $\bar{n}a$ as a function of $\bar{\beta}$ for the case of no impurities. This curve was obtained from HERMES. The stable portion to the right of the minimum was determined by letting an ignited plasma reach a steady-state. The unstable portion was estimated by comparing the α-particle heating and the plasma losses.

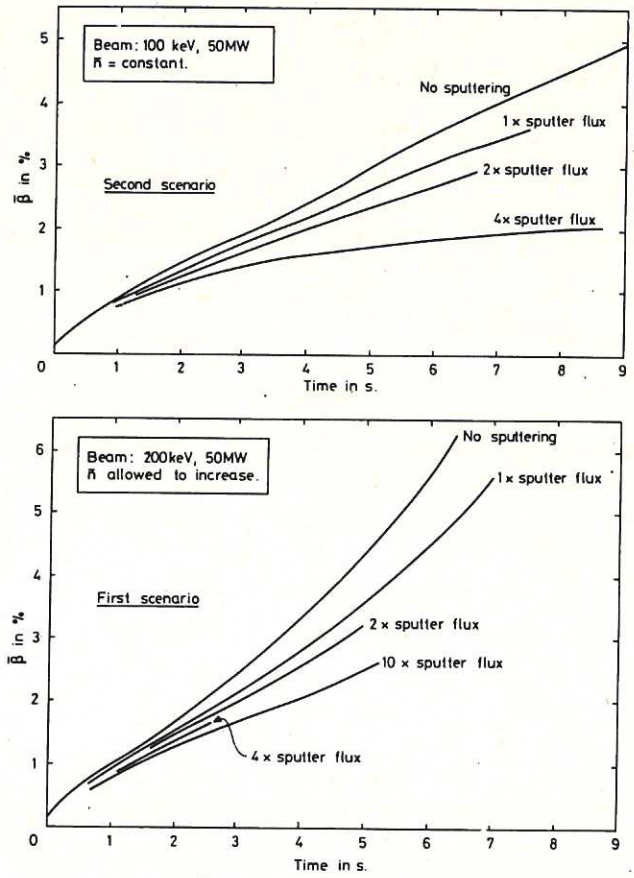

Fig.2 Mean β-value against time for the two scenarios. The flux of sputtered iron atoms has been multiplied by 1,2,4 or 10 to determine the sensitivity of the results to the sputtering model.

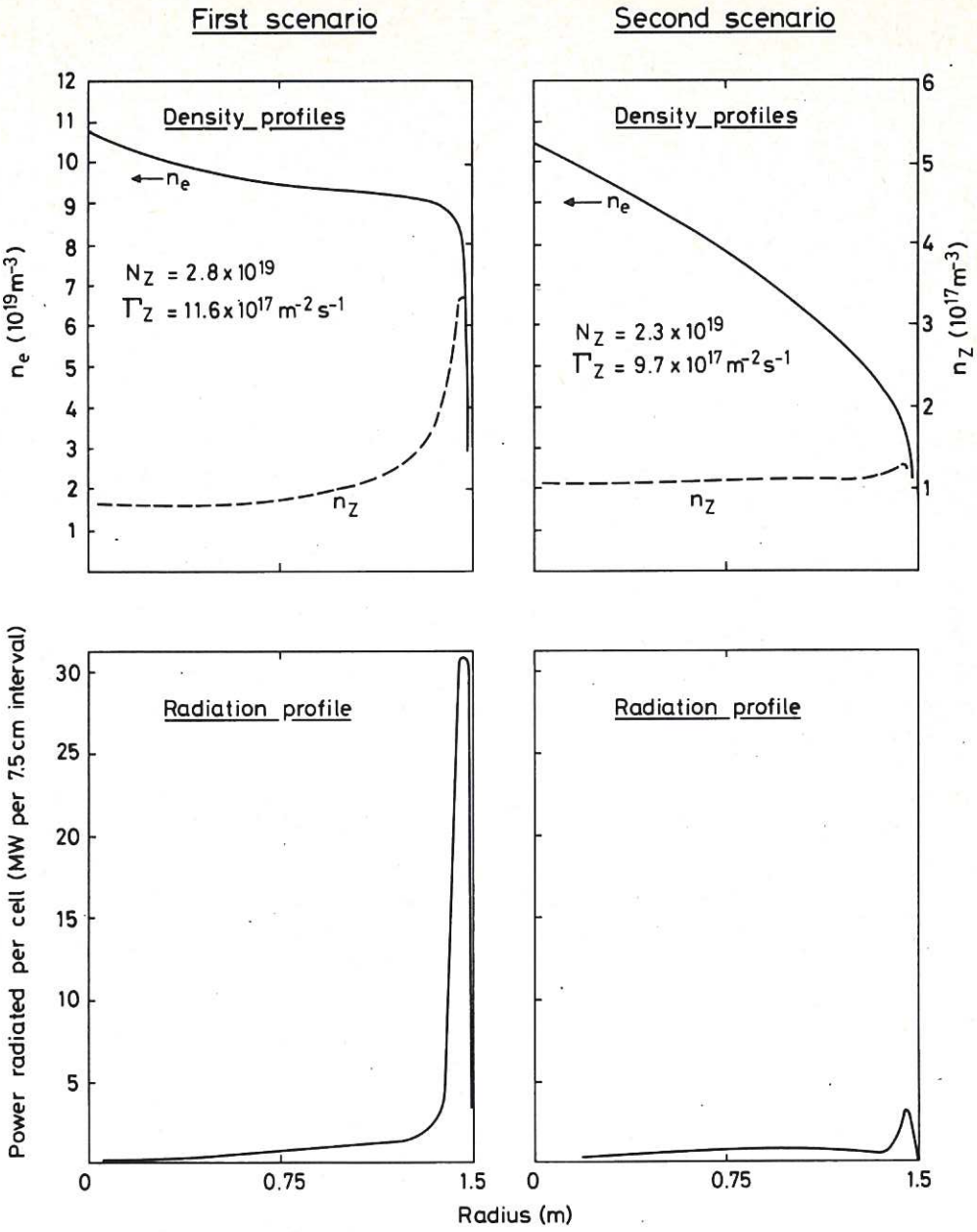

Fig.3 Density and radiation profiles 5 s after start of injection for the two scenarios.

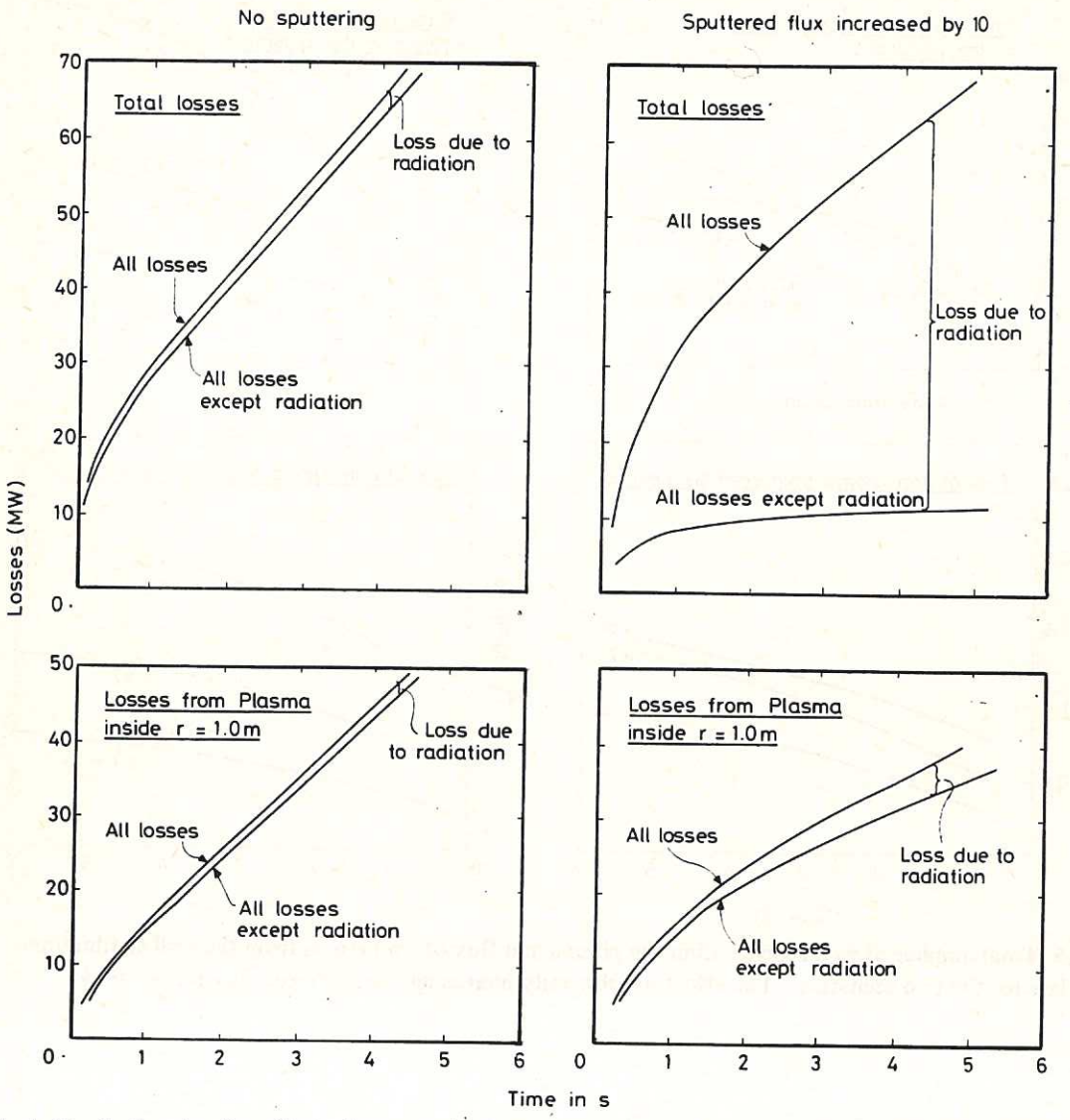

Fig.4 Graph showing the effect of sputtered iron atoms on the radiative losses. In the case where sputtering is present the flux has been increased by a factor 10. Note that the presence of sputtered iron atoms results in radiation being the dominant loss channel from the plasma as a whole. However from plasma inside r = 1·0 m non-radiative mechanisms (e.g. electron conduction) are dominant.

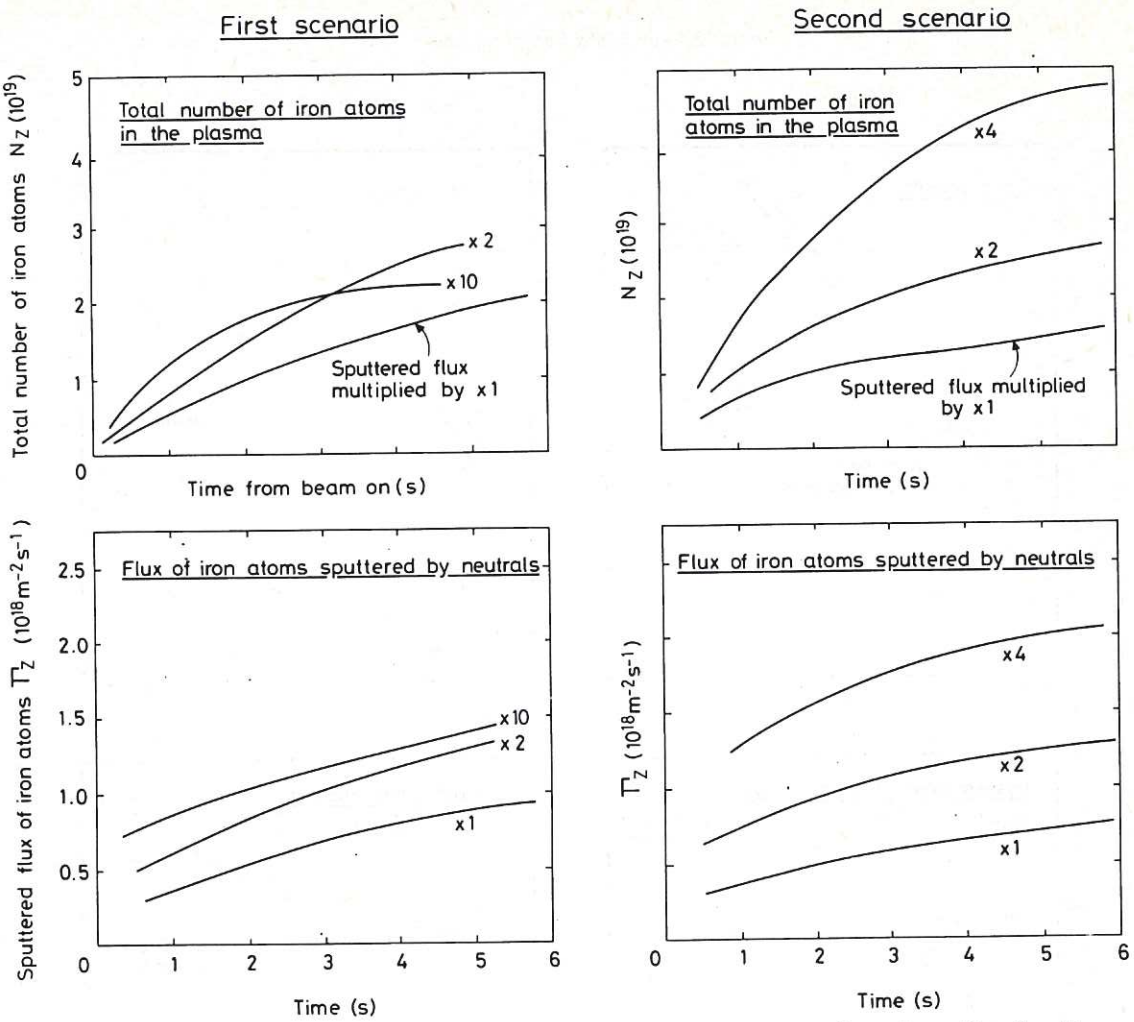

Fig.5 Total number of iron atoms within the plasma and flux of iron atoms from the wall as functions of time for the two scenarios. The effect of arbitrarily increasing the sputtered flux is also shown.

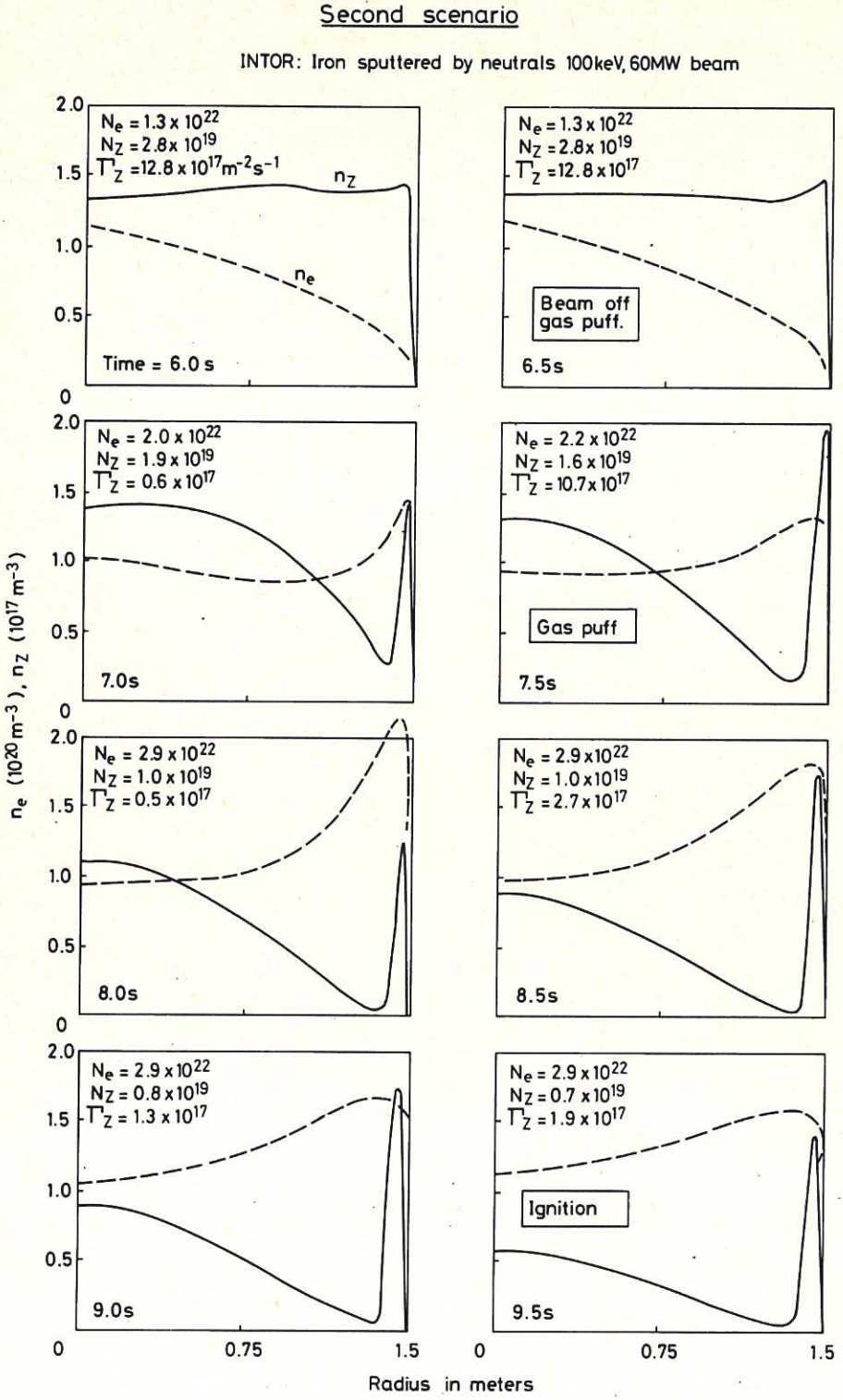

Fig.6 Profiles of n_e and n_Z during the final ignition phase for the second scenario where $\bar{n}$ is held constant while the beam is on. The beam is switched off at 6·5 s and the density progressively increased to take $\bar{n}a$ above the ignition curve.

HER MAJESTY'S STATIONERY OFFICE

Government Bookshops

49 High Holborn, London WC1V 6HB
13a Castle Street, Edinburgh EH2 3AR
41 The Hayes, Cardiff CF1 1JW
Brazennose Street, Manchester M60 8AS
Wine Street, Bristol BS1 2BQ
258 Broad Street, Birmingham B1 2HE
80 Chichester Street, Belfast BT1 4JY

Government publications are also available through booksellers